Sub-grid modeling of coupled hydrodynamic, vegetative and morphodynamic processes in a salt marsh environment

Mithun Deb[1] James T. Kirby[1] Ali Abdolali[2] Fengyan Shi[1]

1 Center for Applied Coastal Research, University of Delaware

2 National Oceanic and Atmospheric Administration

ICCE 2018

36TH INTERNATIONAL CONFERENCE ON COASTAL ENGINEERING 2018

Baltimore, Maryland | July 30 – August 3, 2018

The State of the Art and Science of Coastal Engineering

Motivations

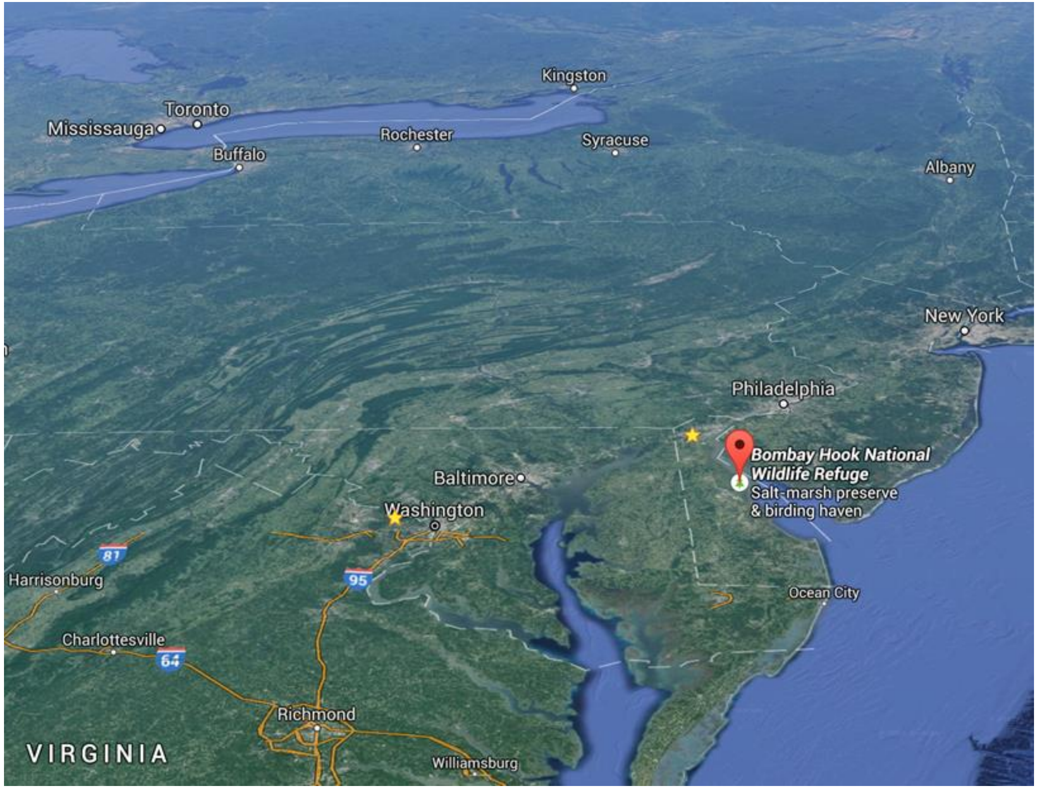

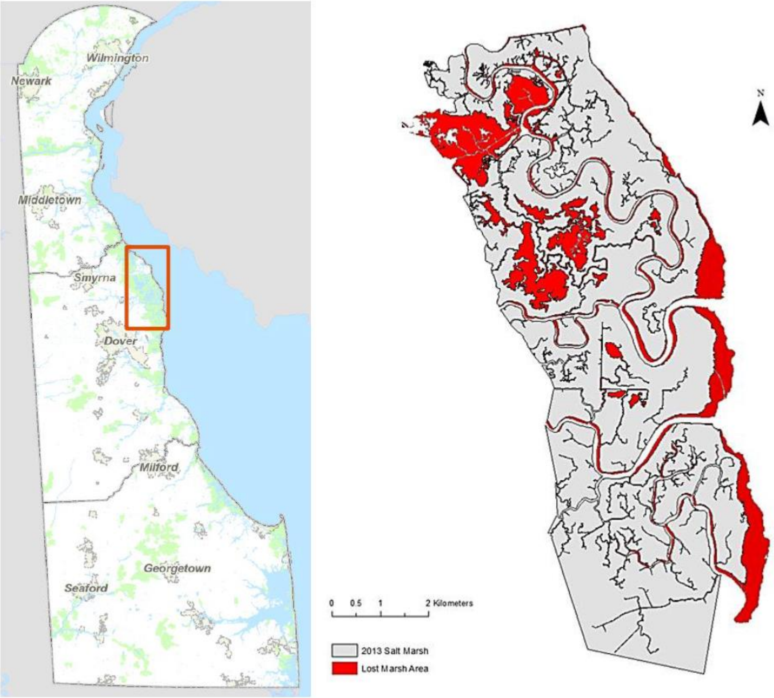

Salt marsh loss in the BHNWR area

[figure: McDowell and Sommerfield (2016)]

Motivations

INTERNAL MARSH LOSS AT BOMBAY HOOK NWR

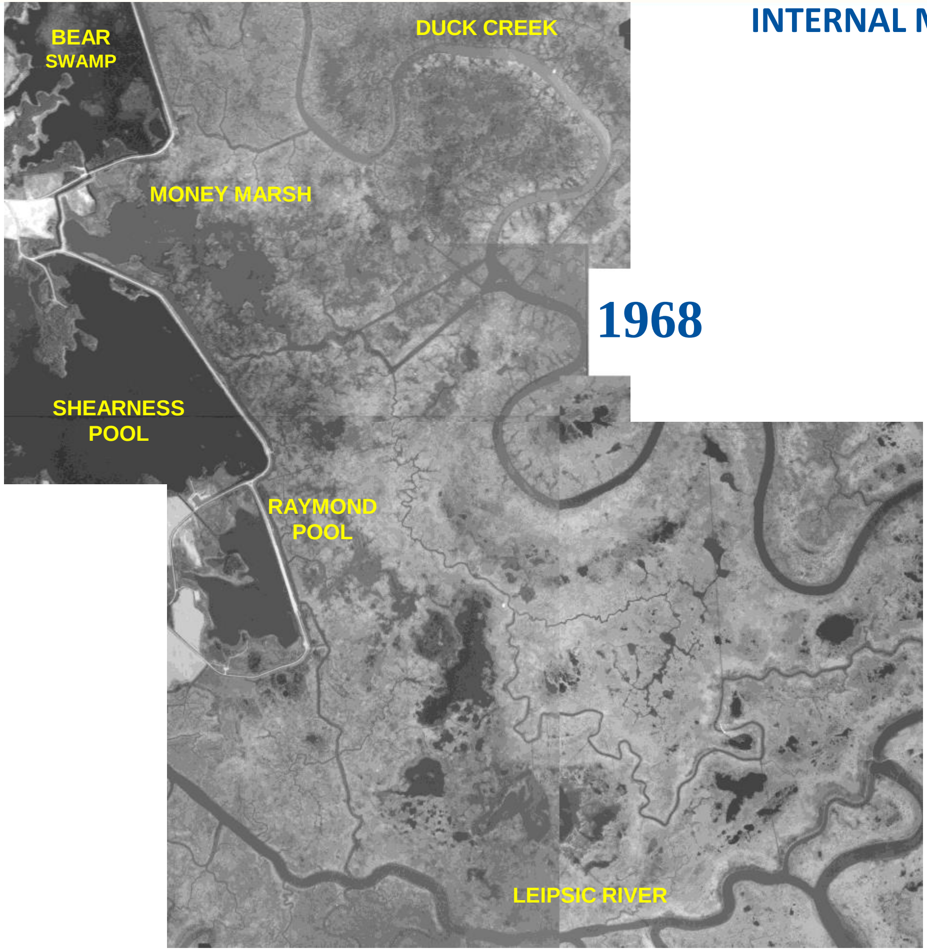

1968

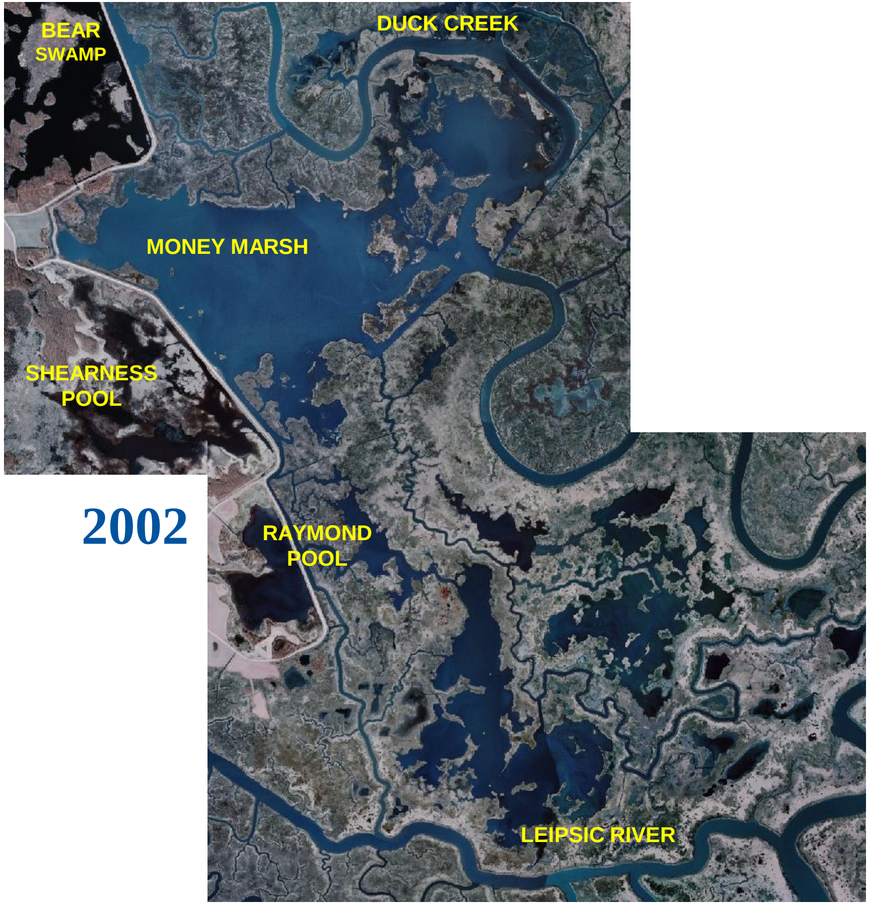

2002

Objectives

Conduct a comprehensive numerical and field investigation to understand:

- The dominant hydrodynamics for present marsh conditions
- Wave climate in the tidally-inundated flat and long term potential for wind wave-driven shoreline erosion
- Net sediment transport (importing/exporting)
- Coupled hydrodynamic, vegetative and morphodynamic processes

A significant hydrodynamic modeling limitation: artificial ponding over the marsh platforms

DEM development

UNIVERSITY OF DELAWARE

TOPOGRAPHY

Present Grid:
2007 & 2011

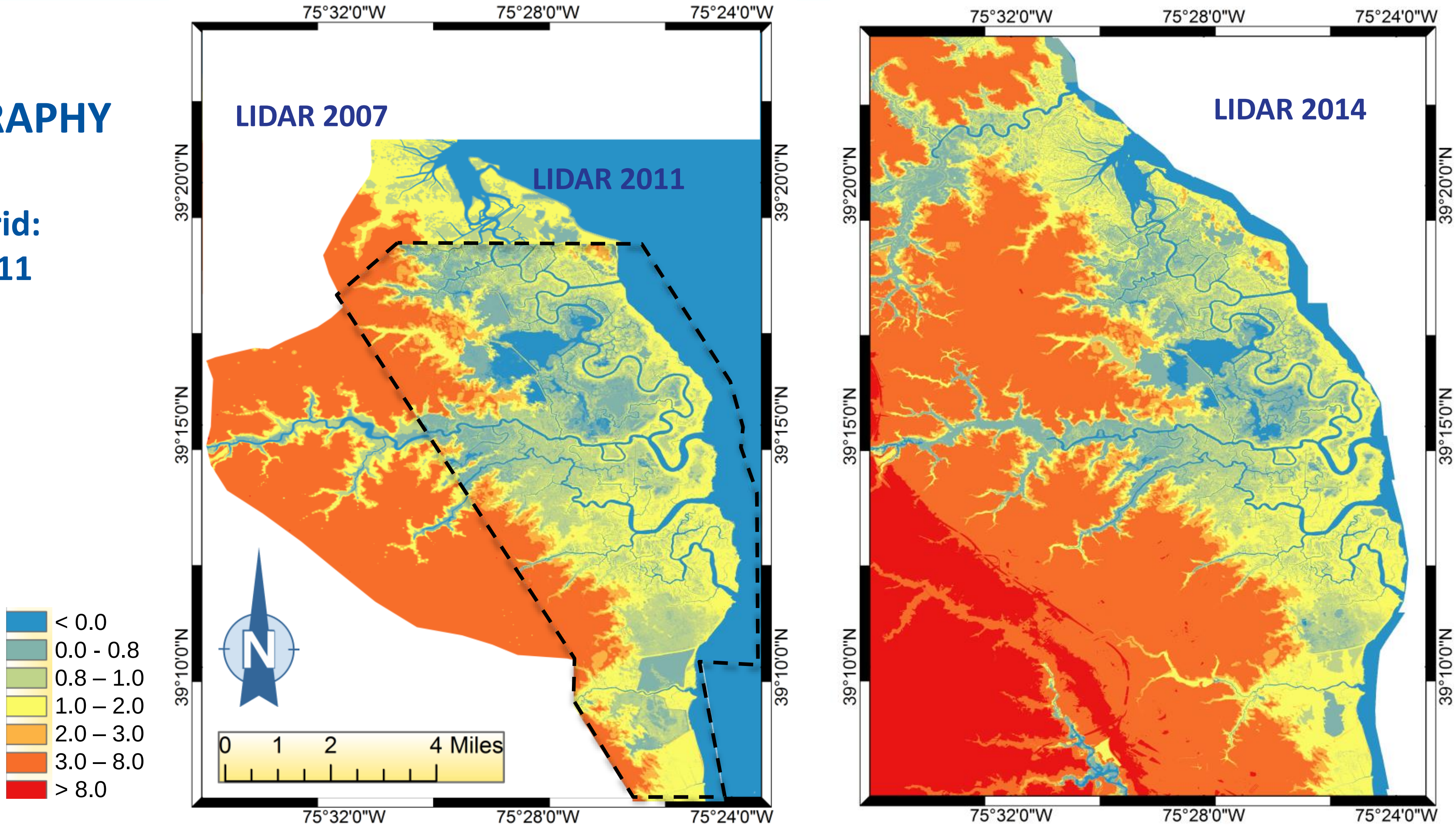

DEM development

LIDAR Comparison

1300 points collected during a ground truth survey

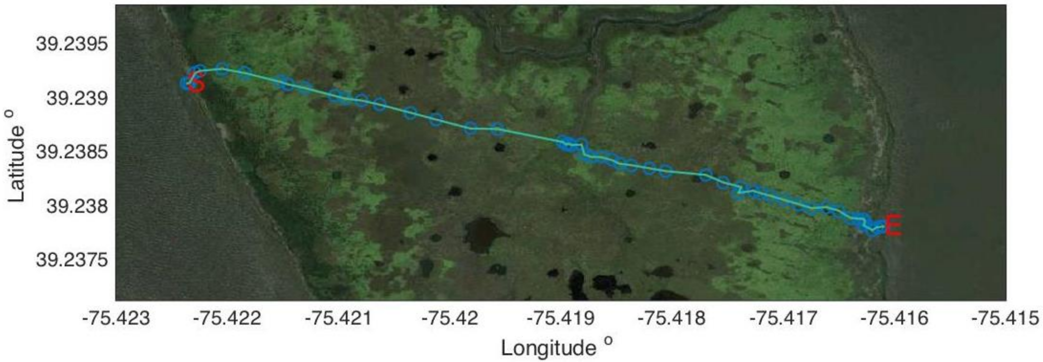

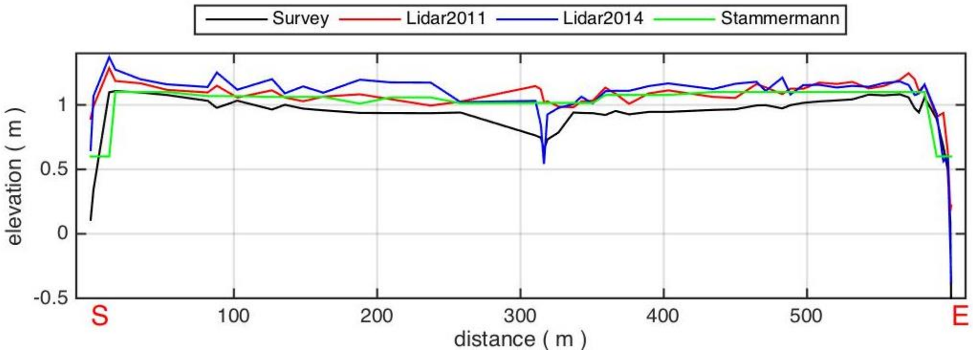

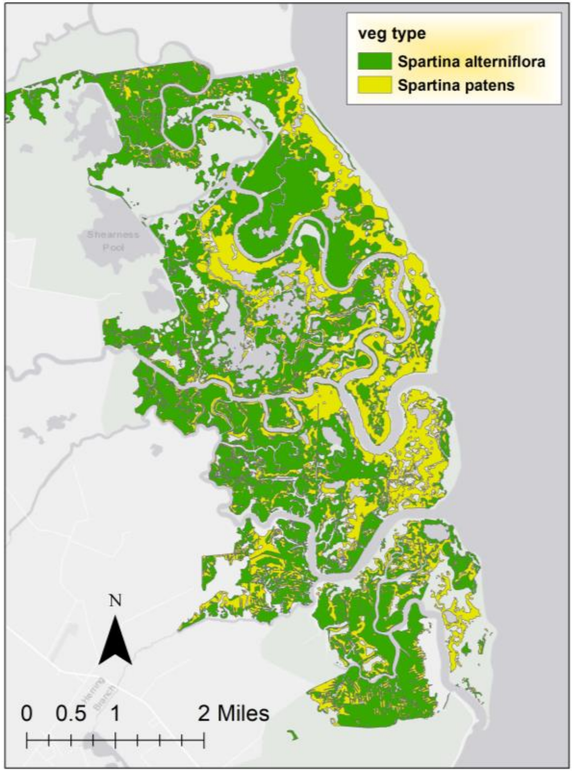

vegetation bias correction

Unstructured Grid

NODES: 370629, CELLS: 740776
FINEST RESOLUTION: 3.5 m

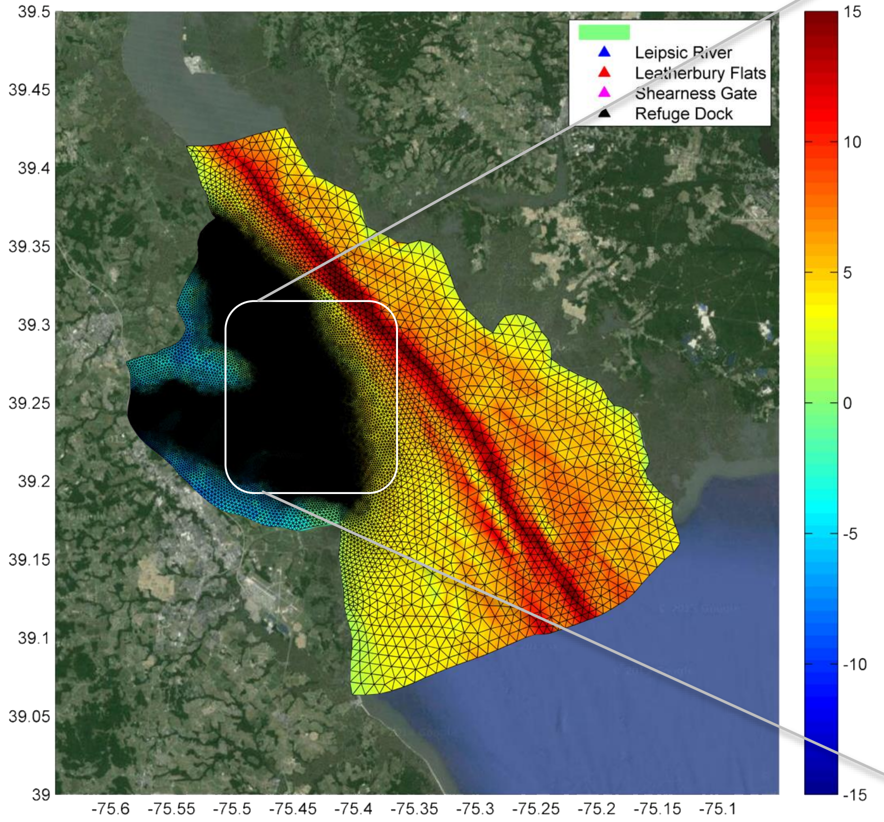

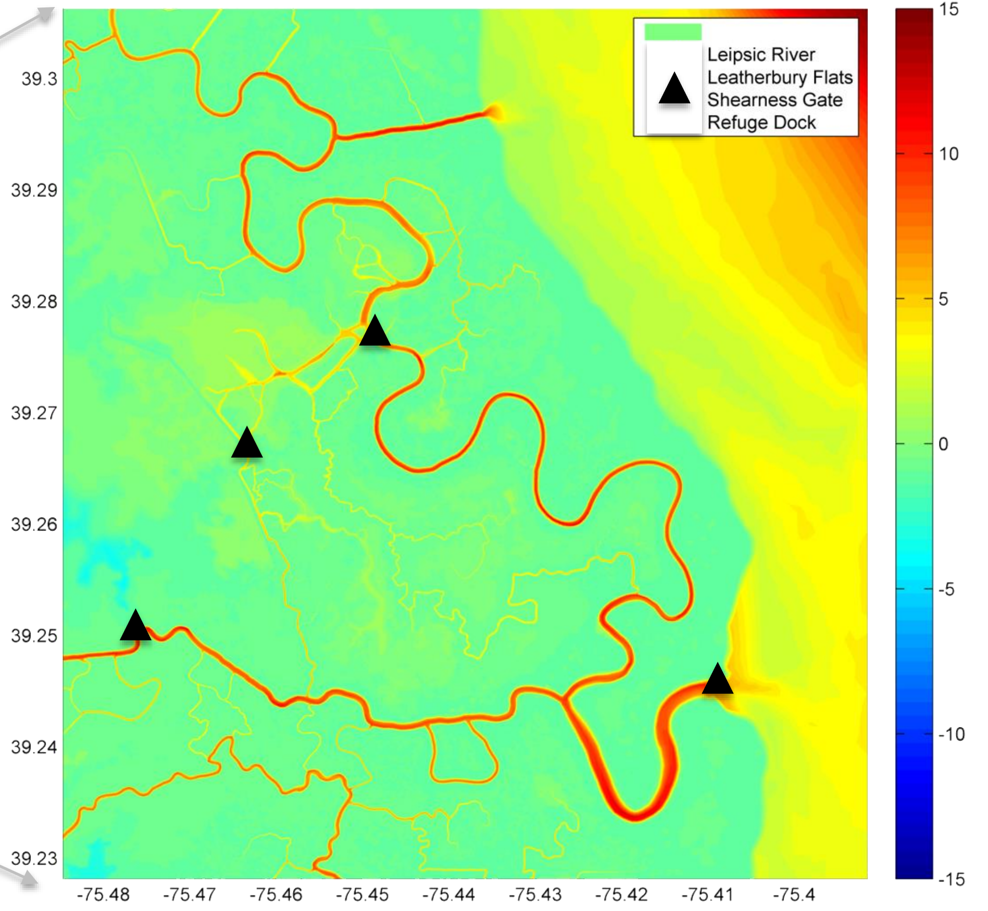

Hydrodynamic Models

FORCING BOUNDARY CONDITION

FVCOM domain

ROMS domain

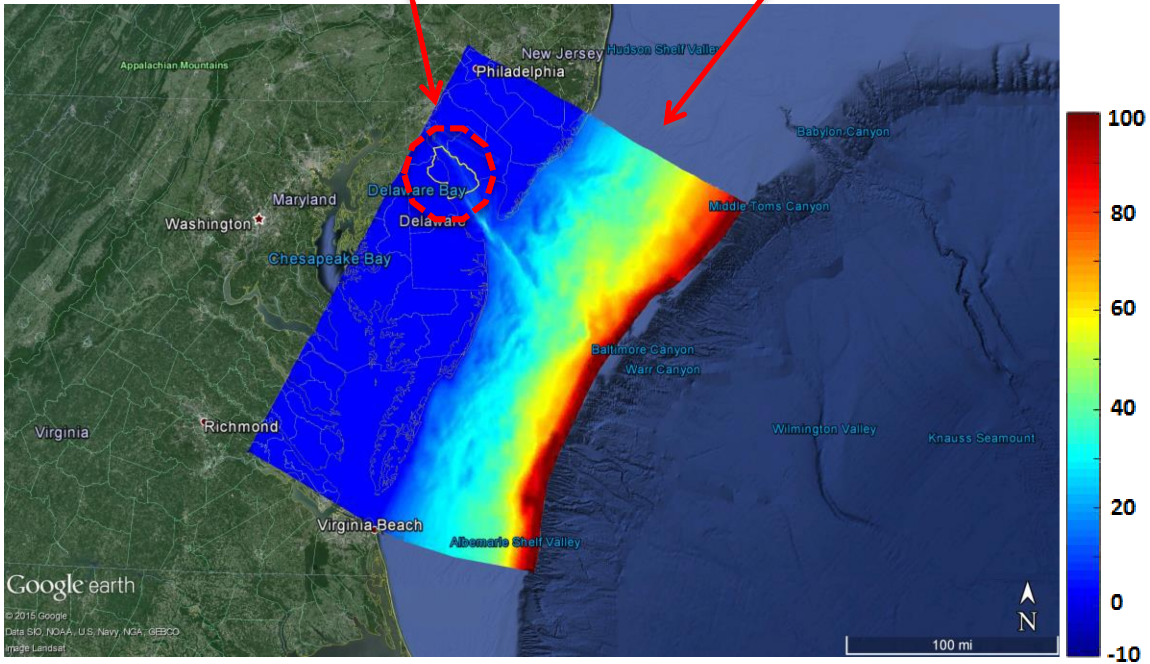

Regional Ocean Modeling System (ROMS)

150 ×300 × 10 structured grid

Forcing Boundaries:

- ✓ Amplitudes and phases for 9 tidal constituents from ADCIRC (M2, S2, M4, M6, K2, K1, N2, O1, and Q1)
- ✓ Wind stress calculated from North American Mesoscale Forecast System (NAM-ANL)
- ✓ River discharge from USGS (extrapolated from Trenton gauge)

.

Finite Volume Community Ocean Model (FVCOM)

Nodes: 370629, Cells: 740776

Forcing Boundaries:

- ✓ Current and Free Surface Elevation from ROMS

.

Model validation

surface elevation

FVCOM model comparison (at Bay and channel tide gauges)

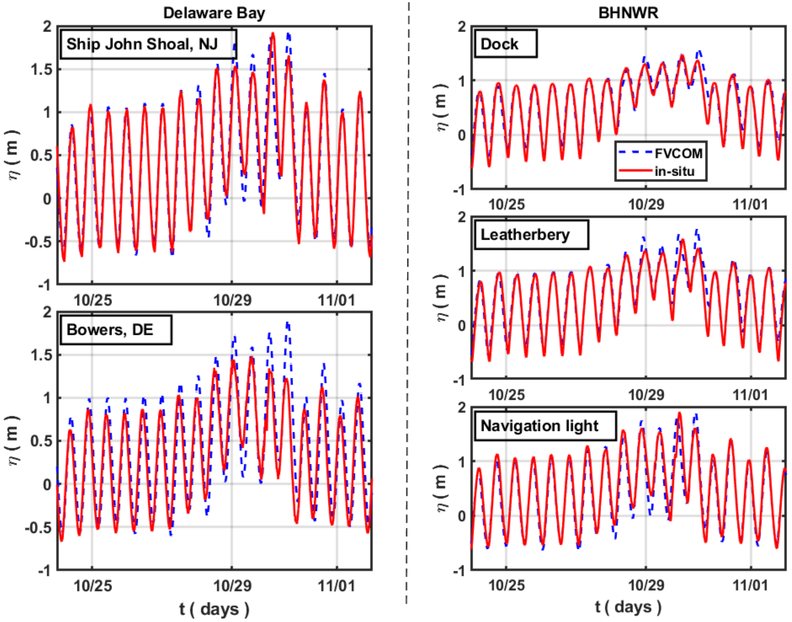

During Hurricane Sandy, 2012

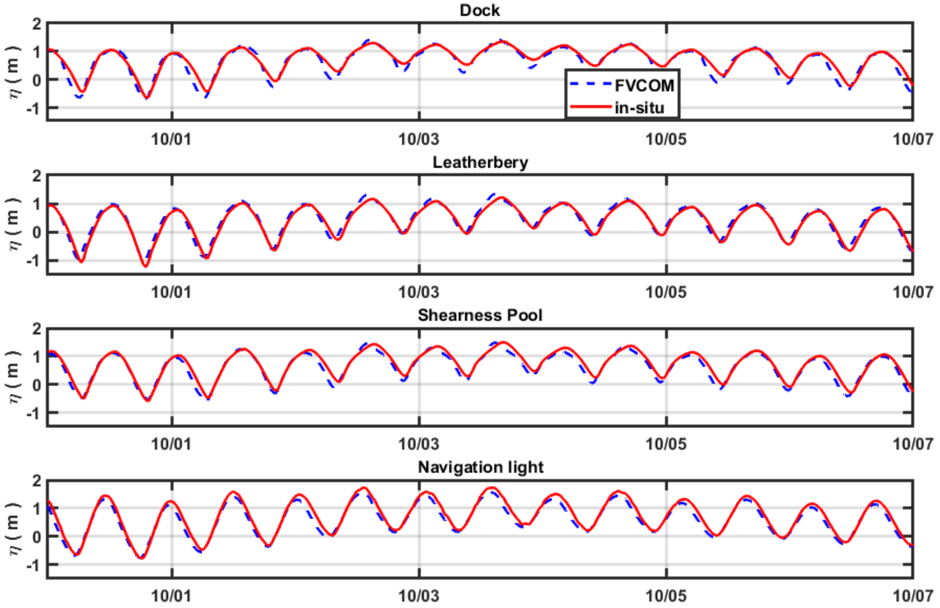

During September storm, 2015

Model validation

FVCOM model comparison (at marsh platform)

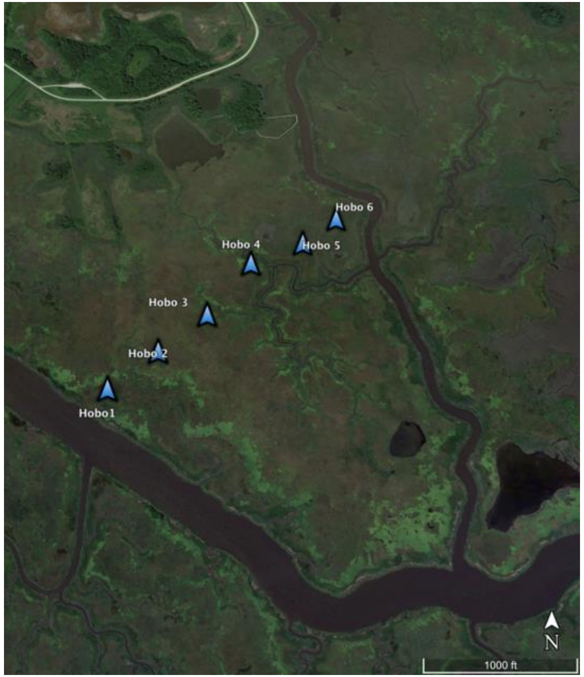

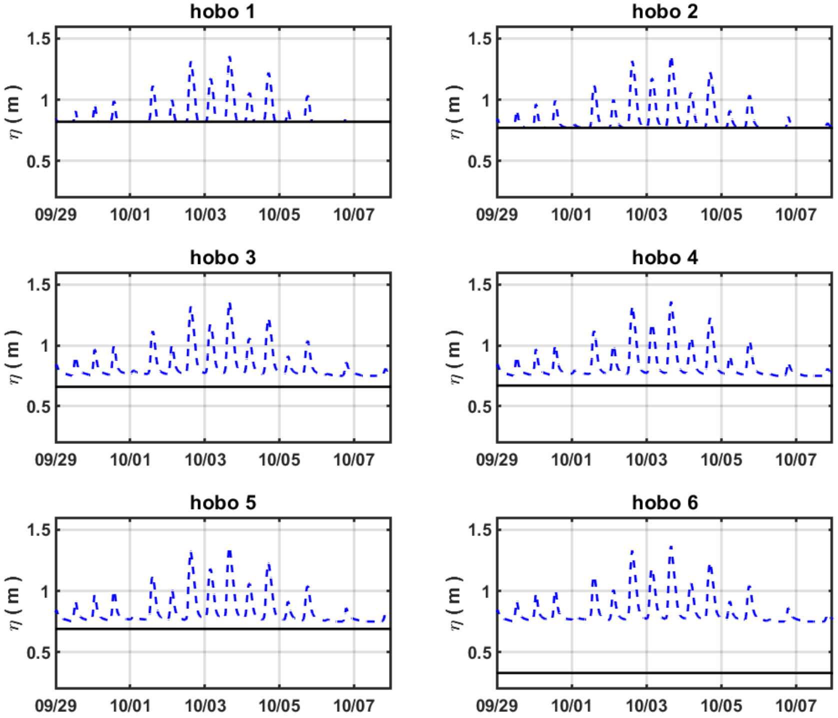

During September storm, 2015

Model grid elevation (black straight line)

Artificial ponding

Total volume of water going in and out of BHNWR

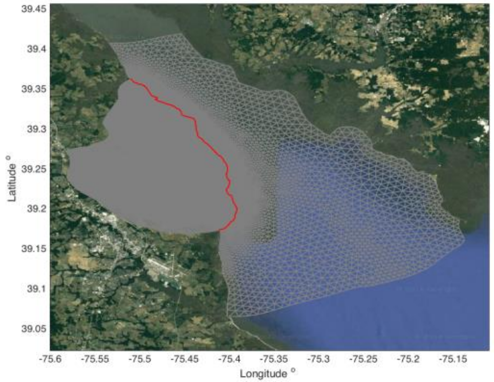

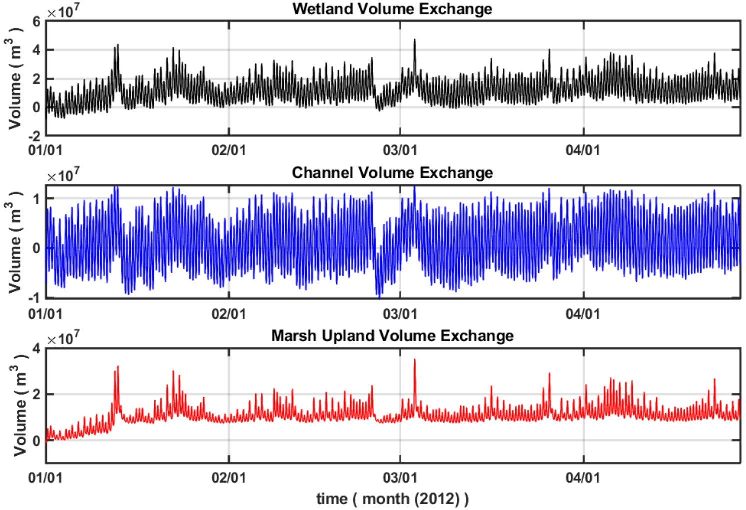

Ongoing work

- Treatment of artificial ponding over marsh platforms

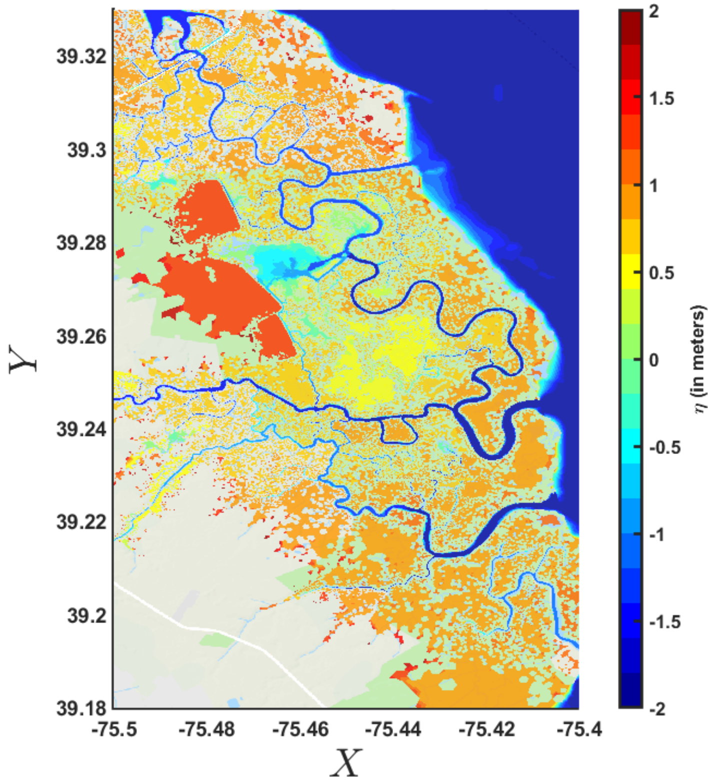

Artificial ponding

Identifying the marsh depressions

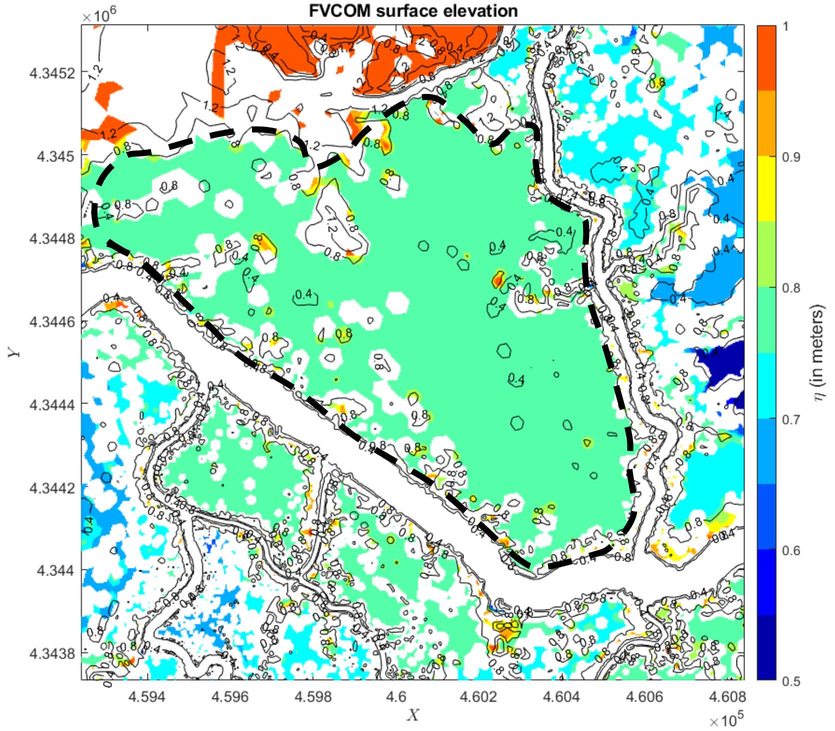

Idealized case

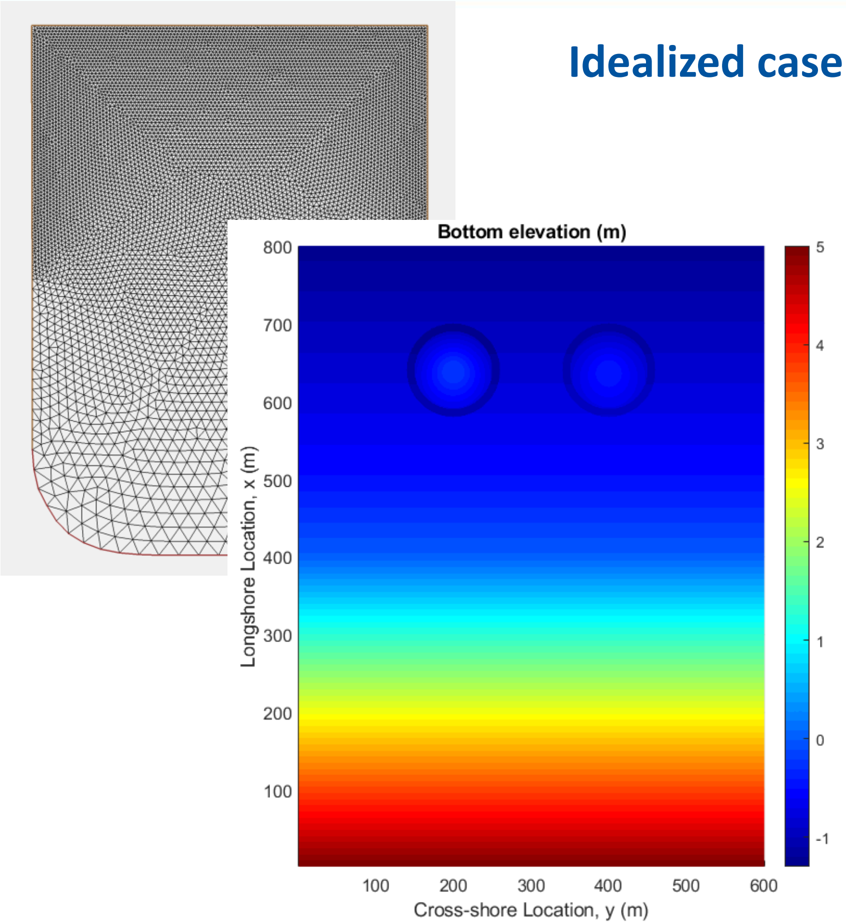

Artificial ponding

Identifying the marsh depressions

surface elevation **wet/dry mask**

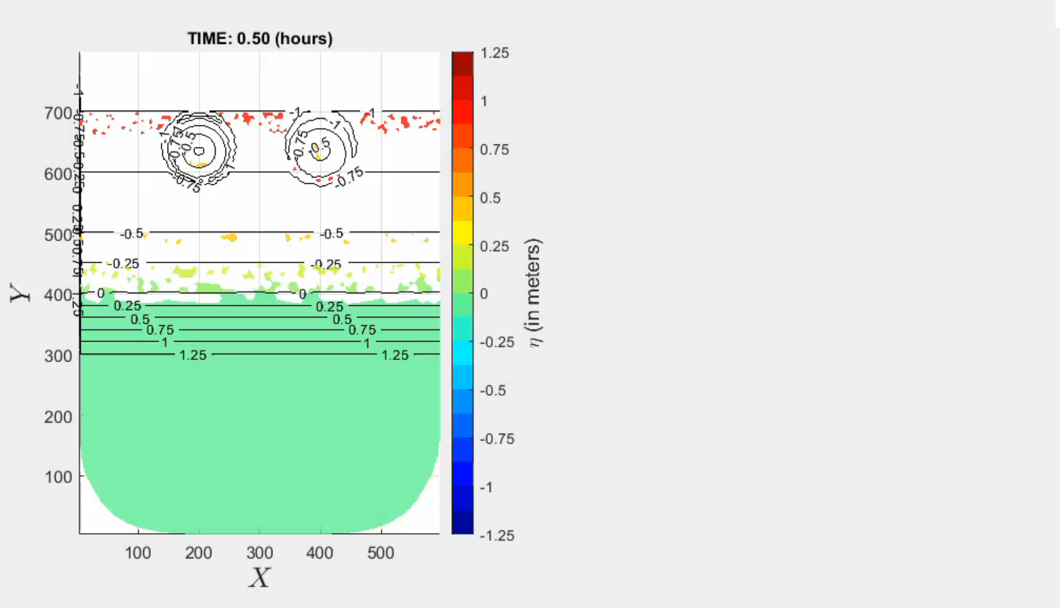

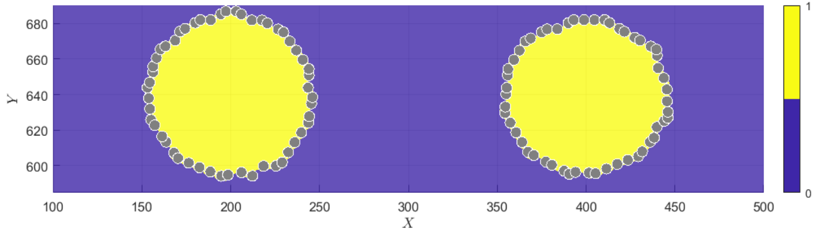

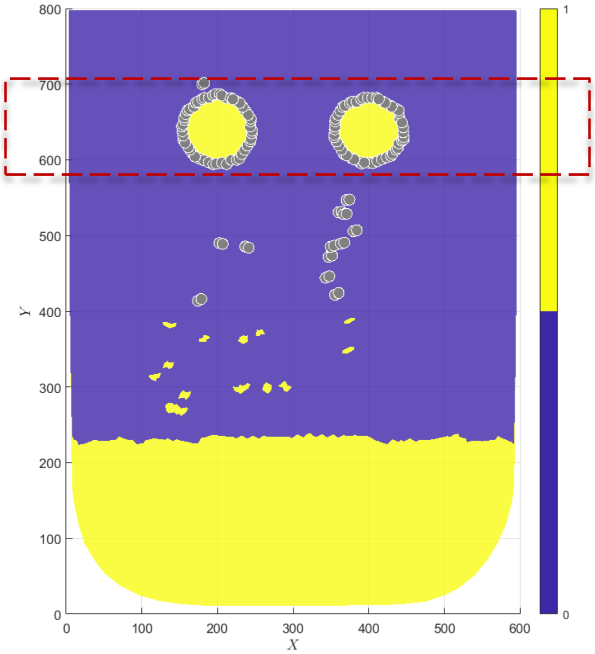

Artificial ponding

Development of Sub-grid Equations

- Defina (2000): Volume averaging

$$\Theta\frac{\partial \eta}{\partial t}+\frac{\partial P}{\partial x}+\frac{\partial Q}{\partial y}=0$$

$$\frac{\partial P}{\partial t}+\frac{\partial}{\partial x}\left(\epsilon_{xx}\frac{P^2}{Y}\right)+\frac{\partial}{\partial y}\left(\epsilon_{xy}\frac{PQ}{Y}\right)+gY\frac{\partial \eta}{\partial x}-\frac{\partial R_{xx}}{\partial x}-\frac{\partial R_{xy}}{\partial y}-\frac{\tau_{sx}}{\rho}+\frac{\tau_{bx}}{\rho}=0$$

$$\frac{\partial Q}{\partial t}+\frac{\partial}{\partial x}\left(\epsilon_{xy}\frac{PQ}{Y}\right)+\frac{\partial}{\partial y}\left(\epsilon_{yy}\frac{Q^2}{Y}\right)+gY\frac{\partial \eta}{\partial y}-\frac{\partial R_{yx}}{\partial x}-\frac{\partial R_{yy}}{\partial y}-\frac{\tau_{sy}}{\rho}+\frac{\tau_{by}}{\rho}=0$$

Porosity :

$$\Theta=\frac{1}{A}\iint_A \varphi|_{z=\eta}\,dA$$

Effective water depth :

$$Y=\frac{1}{A}\int_{-h}^{\eta}\iint_A \varphi\,dA\,dz$$

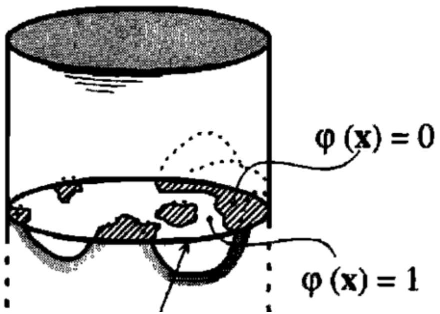

- 2-D equations that solves partially wet elements
- Stochastic representation of porosity parameter for the Venice lagoon

Artificial ponding

Development of Sub-grid Equations

Deterministic case

- Volp et al. (2013): Treatment of friction slope
  - Unidirectional flow within a coarse grid cell
  - Uniform friction slope in a coarse grid cell
- Wu et al. (2016): Pre-storage of volume averages

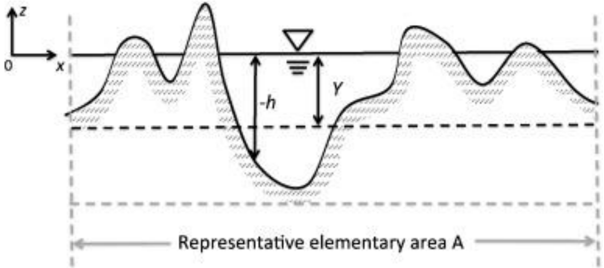

$$\varphi(\mathbf{x}) = \begin{cases} 1 & z > -h \\ 0 & z \leq -h \end{cases}$$

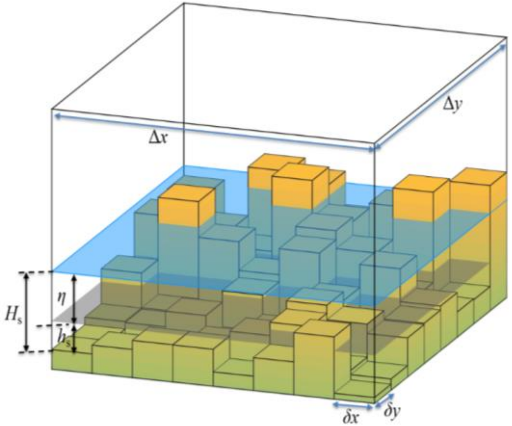

Porosity : $\Theta = \frac{1}{A} \iint_A \varphi|_{z=\eta} dA$

Effective water depth : $Y = \frac{1}{A} \int_{-h}^{\eta} \iint_A \varphi dA dz$

Artificial ponding

Sub-grid simulation at Hobo gauge locations (Stochastic case)

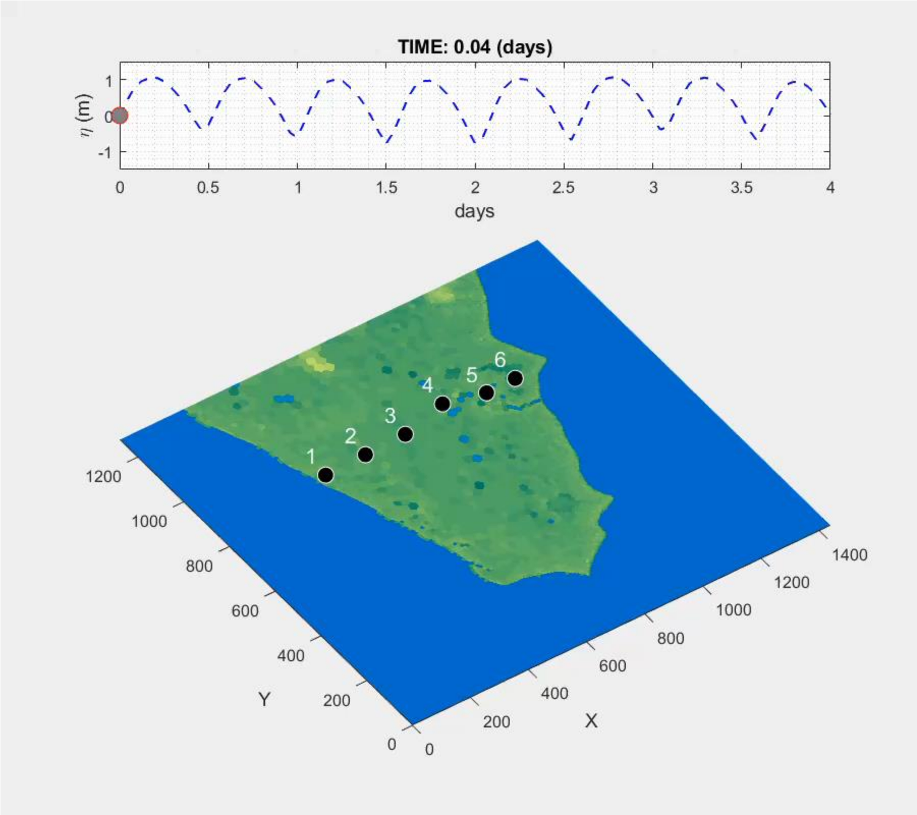

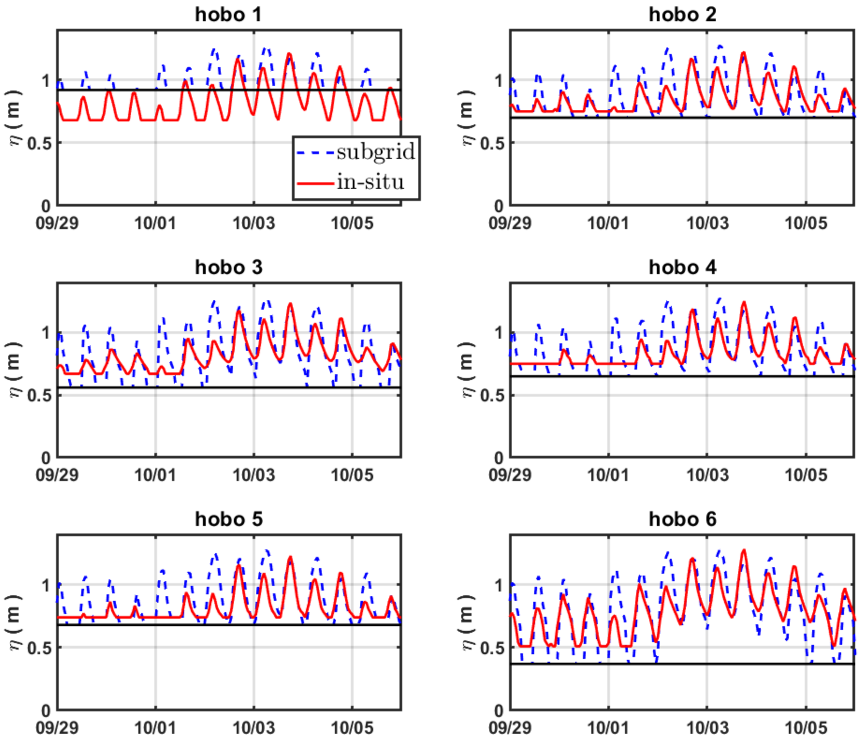

Artificial ponding

Slot method in FVCOM (future work)

- Kennedy et al. (2000), Chen et al. (2000)

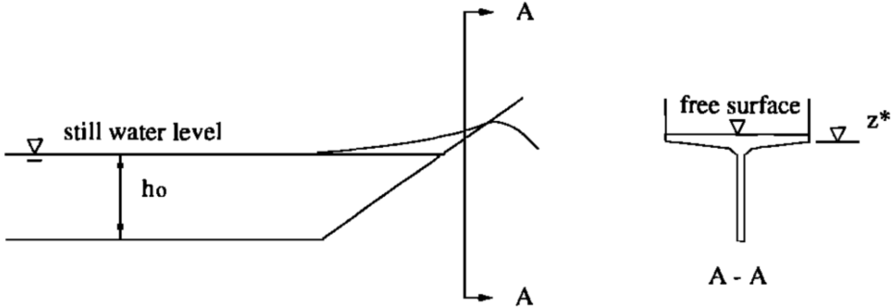

elevation at the top of the slot

$$z^* = \frac{-h}{1-\delta} + h_0\left(\frac{\delta}{1-\delta} + \frac{1}{\lambda}\right)$$

width of the plume

$$b(\eta) = \begin{cases} 1, & \eta \geq z^* \\ \delta + (1-\delta)e^{\lambda(\eta - z^*)/h_0}, & \eta \leq z^* \end{cases}$$

$$\beta\eta_t + \nabla\cdot\mathbf{M} = 0$$

where

$$\mathbf{M} = \Lambda\left[\mathbf{u}_\alpha + \left(\frac{z_\alpha^2}{2} - \frac{1}{6}(h^2 - h\eta + \eta^2)\right)\nabla(\nabla\cdot\mathbf{u}_\alpha) + \left(z_\alpha + \frac{1}{2}(h - \eta)\right)\nabla(\nabla\cdot(h\mathbf{u}_\alpha))\right]$$

Ongoing work

- *Improvement of the FVCOM model with narrow slot approach*
- *Implementing the subgrid model with vegetation and morphodynamic module for long-term morphology changes*

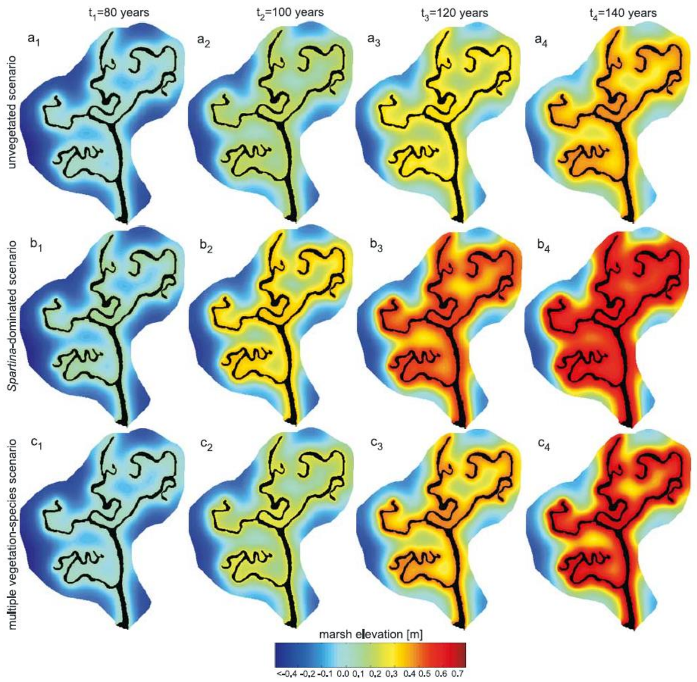

figure from D'Alpaos et al. (2007)

Money Marsh, Bombay Hook National Wildlife Refuge (January, 2016)

Supplemental info

References

Chen, Q., Kirby, J. T., Dalrymple, R. A., Kennedy, A. B., and Chawla, A. (2000). Boussinesq modeling of wave transformation, breaking, and runup. II: 2D. Journal of Waterway, Port, Coastal, and Ocean Engineering, 126(1), 48-56.

D'Alpaos, A., Lanzoni, S., Marani, M. and Rinaldo, A. (2007). Landscape evolution in tidal embayments: Modeling the interplay of erosion sedimentation and vegetation dynamics, J. Geophys. Res., 112, F01008.

Defina, A. (2000) Two-dimensional shallow flow equations for partially dry areas. Water Resources Research, 36(11), 3251.

Kennedy, A. B., Chen, Q., Kirby, J. T., and Dalrymple, R. A. (2000). Boussinesq modeling of wave transformation, breaking, and runup. I: 1D. Journal of waterway, port, coastal, and ocean engineering, 126(1), 39-47.

McDowell, C. and Sommerfield, C. (2016) Geomorphic analysis of Bombay Hook NWR. DE Wetlands Conference 2016,Wilmington, DE.

Shi, F., Kirby, J. T., Wu, G., Abdolali, A. and Deb, M. (2016) Subgrid modeling of geomorphological and ecological processes in salt marsh evolution, AGU Fall Meeting, Abstract OS21C-04, San Francisco.

Wu, G et al. (2016) A pre-storage, subgrid model for simulating flooding and draining processes in salt marshes, Coastal Engineering, 108, 65-78.

Hydrodynamic Models

Forcing boundary condition

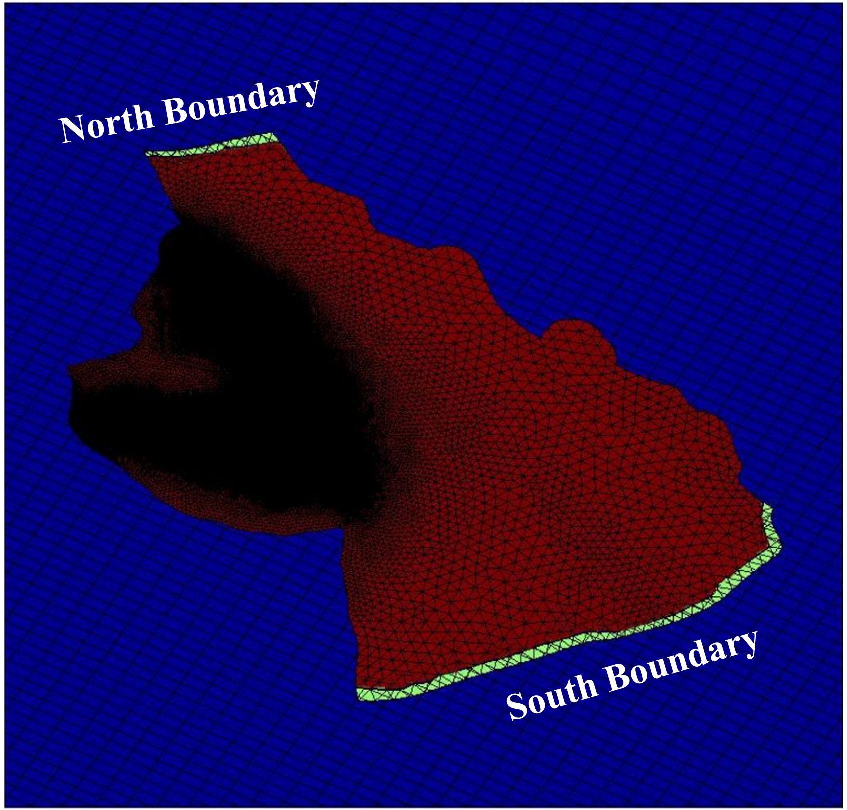

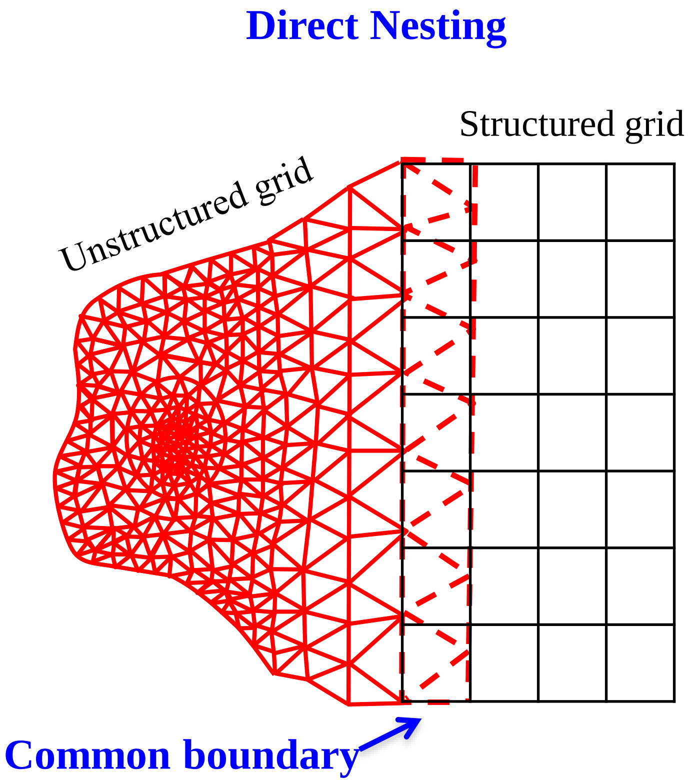

Velocity: Coarse grid vs. Subgrid

Assumptions：within a coarse grid

1. Unidirectional flow
2. Constant friction slope

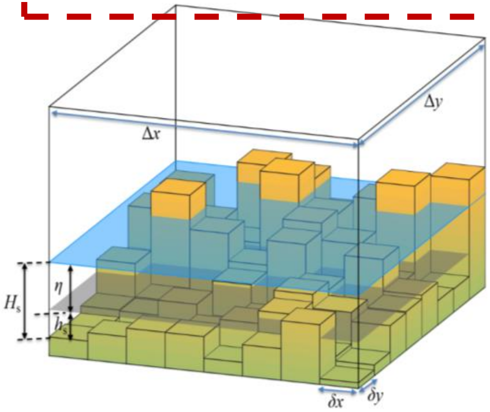

Velocity at coarse grid：

$$u = \frac{1}{AY} \iint_A H_s u_s dA$$

Relation between velocities at coarse grid and subgrid

$$(u_s, v_s) = \frac{(u, v)}{\alpha_s}$$

where $\alpha_s = \frac{\sqrt{C_{ds}/H_s}}{AY} \iint_A H_s \sqrt{H_s/C_{ds}} dA$

Pre-storage Method

Lookup tables for

Porosity at surface

$$\Theta = \frac{1}{A}\iint_A \varphi|_{z=\eta} dA$$

Effective water depth

$$Y = \frac{1}{A}\int_{-h}^{\eta}\iint_A \varphi dA dz$$

Equivalent friction coefficient

$$C_d = \frac{1}{A}\iint_A \frac{H_s}{H_f} dA$$

$Q(h), Y(h), Cd(h)$ are obtained by linear interpolation or polynomial fitting method

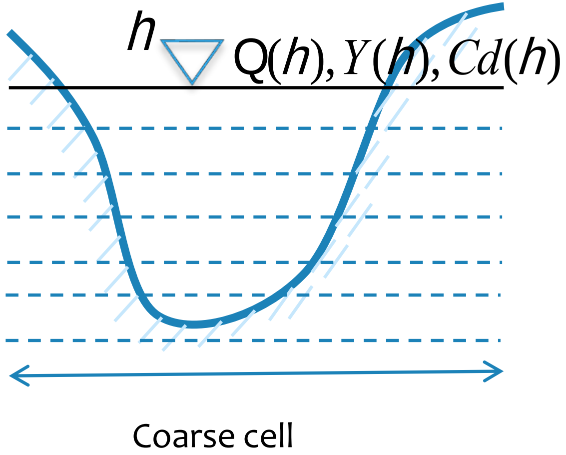

Subgrid Sediment Model

- Sediment Module

$$Y\frac{\partial \bar{c}}{\partial t}+\Theta\bar{c}\frac{\partial \eta}{\partial t}+\frac{\partial \bar{c}P}{\partial x}+\frac{\partial \bar{c}Q}{\partial y}-\left[\frac{\partial}{\partial x}\left(\nu Y\frac{\partial \bar{c}}{\partial x}\right)+\frac{\partial}{\partial y}\left(\nu Y\frac{\partial \bar{c}}{\partial y}\right)\right]-S=0$$

$$S=E-D=\iint_{A_{\mathrm{wet}}} E_s \mathrm{d}A-\iint_{A_{\mathrm{wet}}}(D_s+D_{tp})\mathrm{d}A$$

erosion deposition

$$E_s=\begin{cases} M\left(\frac{\tau_s}{\tau_{ce}}-1\right) & \tau_s>\tau_{ce} \\ 0 & \tau_s\le\tau_{ce}\end{cases}$$

$$D_s=\begin{cases} \omega_s c_s\left(1-\frac{\tau_s}{\tau_{cd}}\right) & \tau_s<\tau_{ce} \\ 0 & \tau_s\ge\tau_{cd}\end{cases}$$

$$D_{tp}=c_s U\epsilon d_s n_s \min(h_s, H)$$

$$\epsilon=\alpha_\epsilon\left(\frac{Ud_s}{\nu}\right)^{\beta_\epsilon}\left(\frac{d_{50}}{d_s}\right)^{\gamma_\epsilon}$$

$$\rho_b\frac{\partial Z_b}{\partial t}+\frac{f_{\mathrm{mor}}}{1-p_b}\left(E-D-D_{bg}\right)=0$$

Organic deposition: $D_{bg}=D_{bg,0}\frac{B}{B_{\max}}$

Friction: Coarse grid vs. sub-grid

Total bottom friction

$$\tau_{\mathbf{b}} = \frac{\rho}{A} \iint_A C_{ds} \left| \mathbf{u_s} \right| \mathbf{u_s} dA, \quad \text{with} \left| \mathbf{u_s} \right| = \sqrt{u_s^2 + v_s^2}$$

$$\tau_{bx} = \frac{\rho u |\mathbf{u}|}{A} \iint_A \frac{C_{ds}}{\alpha_s^2} dA$$

$$= \rho C_d u |\mathbf{u}|$$

Effective friction coefficient C_d, *frictional depth* H_f

$$C_d = \frac{1}{A} \iint_A \frac{H_s}{H_f} dA \qquad H_f = \left[\frac{\iint_A H_s \sqrt{H_s / C_{ds}} dA}{AY} \right]^2$$

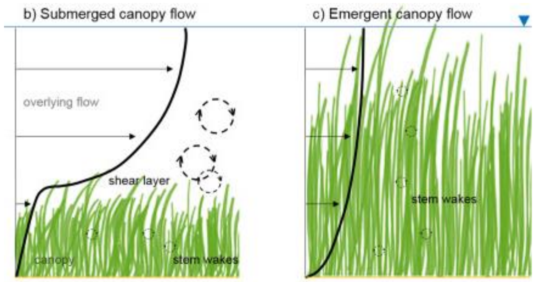

In Wu et al., 2017

Vegetation-induced friction

$${}_x = \frac{u|\mathbf{u}|}{A} \iint_A \frac{2C_b + C_D \ {}_s n_s H_s}{2\alpha_s^2} \mathrm{d}A$$